

# A Computational Study on the Interaction of the Nitric Oxide Ions NO<sup>+</sup> and NO<sup>-</sup> with the Side Groups of the Aromatic Amino Acids

Jesse J. Robinet, Cristina Baciu, Kyung-Bin Cho,<sup>†</sup> and James W. Gauld\*

Department of Chemistry and Biochemistry, University of Windsor, Windsor, Ontario N9B 3P4, Canada

Received: July 27, 2006; In Final Form: January 11, 2007

The interaction of the nitric oxide ions NO<sup>+</sup> and NO<sup>-</sup> with benzene (C<sub>6</sub>H<sub>6</sub>) and the aromatic R-groups of the amino acids phenylalanine (Phe), tyrosine (Tyr), histidine (His), and tryptophan (Trp) have been examined using the DFT method B3LYP and the conventional electron correlation method MP2. In particular, the structures and complexation energies of the resulting half-sandwich Ar⋯NO<sup>+/-</sup> and sandwich [Ar⋯NO⋯Ar]<sup>+/-</sup> complexes have been considered. For the Ar⋯NO<sup>+</sup> complexes, the presence of an electron rich heteroatom within or attached to the ring is found to not preclude the cation⋯π bound complex from being the most stable. Furthermore, unlike the anionic complexes, the π⋯cation⋯π ([Ar⋯NO⋯Ar]<sup>+</sup>) complexes do not correspond to a “doubling” of the parent half-sandwich.

## 1. Introduction

Nitric oxide (NO) has long been of interest due in part to its role as an atmospheric pollutant.<sup>1</sup> This interest increased dramatically with the discovery of its *in vivo* synthesis<sup>2</sup> and the ongoing unveiling of its diverse physiological roles as an important secondary messenger molecule.<sup>3</sup> In addition to •NO itself, the nitrosium cation (NO<sup>+</sup>) and nitroxyl anion (NO<sup>-</sup>) are also thought to be responsible for at least some of the diverse functions of nitric oxide.<sup>4–8</sup> Furthermore, some of the roles of these NO species have also been attributed to *S*-nitrosothiols (RSNOs),<sup>9–11</sup> a common form for transporting and delivering NO and its ions around the body. For instance, NO<sup>+</sup> is thought to induce the release of Ca<sup>2+</sup> from smooth muscle in a cGMP-independent manner<sup>4</sup> while the nitroxyl anion, or at least in its protonated form (HNO), is known to be able to modify the activity of some enzymes and receptors.<sup>5</sup> Some of these regulatory roles are achieved via covalent modifications of amino acid residues. Recently, however, it was shown that *S*-nitrosoglutathione (GSNO) can noncovalently interact with aromatic rich regions of proteins and, remarkably, induce structural changes.<sup>12</sup>

Many cations are known to be able to participate in noncovalent interactions with the π-systems of electron rich aromatic compounds.<sup>13,14</sup> Such interactions themselves have been extensively studied and are now known to also be important in an array of physiological functions including the structure and function of proteins.<sup>15–18</sup> In addition to π⋯cation or “half-sandwich” complexes, such interactions may also lead to the formation of π⋯cation⋯π or sandwich complexes. In particular, there is increasing experimental evidence that some proteins contain multiple aromatic rings that interact with a single cation.<sup>14,17</sup> While such species are well-known in organometallic chemistry, their nature and potential roles in biochemical systems are less well understood. Unfortunately, despite their importance, to date there have been relatively few

studies on such species. Furthermore, those studies that have considered related model systems have in general only examined the interactions of cations with simple aromatic species such as benzene, pyrrole, and indole as models of the aromatic amino acids.<sup>17</sup> It has been found that anions can also form analogous anion⋯π complexes if the aromatic species is electron deficient.<sup>19,20</sup> However, it was also determined that the anions may interact by forming hydrogen bonds.<sup>20</sup> In general, this occurs via appropriate substituents such as –OH or –NH– groups. However, C–H bonds are also polarized, although to a lesser extent, and have been found to also be able to participate in hydrogen-bonding.<sup>21,22</sup> Indeed, such interactions have been previously shown to be important in a variety of biological activities.<sup>23,24</sup>

Previously, the interaction of •NO and NO<sup>+</sup> with benzene has been investigated both experimentally<sup>25–28</sup> and computationally.<sup>28–33</sup> In particular, it was found<sup>29</sup> that •NO can interact with the π-system of benzene, though only weakly, while in contrast NO<sup>+</sup> can form strong cation⋯π interactions with aromatic compounds.<sup>28,30–33</sup> However, their interaction and that of NO<sup>-</sup> with biochemically important aromatic biomolecules have not been previously reported. In addition, recent experimental studies by Rosokha et al.<sup>26,27</sup> found that, remarkably, NO<sup>+</sup> is also capable of forming sandwich complexes with aromatic species. However, they suggested that not all arenes were capable of forming such structures.

In this present study we have employed *ab initio* and density functional theory methods in order to investigate the interactions of the biochemically important NO<sup>+</sup> and NO<sup>-</sup> ions with benzene and the aromatic side chains of the amino acids phenylalanine, tyrosine, histidine, and tryptophan (Figure 1). Furthermore, we have also examined the structures and energetics of their corresponding sandwich complexes.

## 2. Computational Methods

All calculations were performed using the Gaussian 03<sup>34</sup> suite of programs. Density functional theory (DFT) calculations were performed using the B3LYP method, a pairing of Becke’s three-parameter hybrid exchange functional<sup>35</sup> as implemented in the

\* To whom correspondence should be addressed. E-mail: gauld@uwindsor.ca.

<sup>†</sup> Current Address: Department of Organic Chemistry, The Hebrew University, Givat Ram Campus, Jerusalem 91904, Israel.

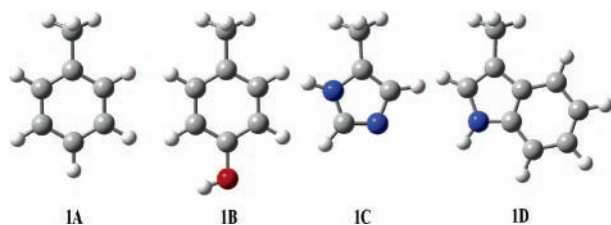


**Figure 1.** Models used in this present study for the side (R-) groups of the aromatic amino acids (**1A**) phenylalanine (Phe), (**1B**) tyrosine (Tyr), (**1C**) histidine (His), and (**1D**) tryptophan (Trp): C (gray); N (blue); O (red); H (white).

above program<sup>36</sup> with the Lee–Yang–Parr correlation functional.<sup>37</sup> Depending on the chemical system, it was used in combination with a variety of Pople basis sets ranging from 6-311G(d,p) to 6-311+G(2df,p) as well as Dunning’s aug-cc-pVDZ and aug-cc-pVTZ basis sets. The latter two basis sets were also used in combination with the ab initio Møller–Plesset second-order perturbation (MP2) method. Restricted methods were used for all closed-shell species and complexes involving NO<sup>+</sup>. Unrestricted methods were used for all open-shell species and complexes with NO<sup>-</sup> due to its ground-state triplet multiplicity. Spin contamination in all unrestricted calculations was negligible, with all  $\langle S^2 \rangle$  values lying in the range 2.007–2.051 (see Table S2 in Supporting Information). In addition, for all complexes the stability of the wave function<sup>38,39</sup> was tested and verified at each level of theory employed. Harmonic vibrational frequencies were obtained at each level of theory except MP2/aug-cc-pVTZ in order to verify that each complex obtained was an energy minimum. Complexation energies were corrected by including the appropriate zero-point vibrational energy (ZPVE), the MP2/aug-cc-pVDZ calculated ZPVE being used for MP2/aug-cc-pVTZ, and basis set superposition error (BSSE) correction as determined using the counterpoise method.<sup>40,41</sup> The resulting energies (kJ mol<sup>-1</sup>) are denoted by  $\Delta E_{\text{corr}}$ . Unless otherwise noted, the abbreviations Phe, Tyr, His, and Trp refer to the models of the respective aromatic amino acids.

### 3. Results and Discussion

**3.1. Assessment of Computational Methods.** In computational studies the size of the chemical system can impose a limit on the choice of method. Ultimately, we wish to investigate large sandwich-type complexes, beyond the tractability of most ab initio methods. Hence, we began by considering the ability of the widely used DFT method B3LYP in conjunction with a variety of basis sets to provide reliable results for aromatic  $\cdots\text{NO}^{+/-}$  systems. The simplest complexes examined as part of this present study were considered, C<sub>6</sub>H<sub>6</sub> $\cdots\text{NO}^{+/-}$ , with the results being compared with those obtained at the conventional MP2/aug-cc-pVTZ level of theory.

**3.2. C<sub>6</sub>H<sub>6</sub> $\cdots\text{NO}^+$  Complexes.** Upon interacting, at all levels of theory, NO<sup>+</sup> binds toward one end of the face of C<sub>6</sub>H<sub>6</sub> with its oxygen directed up and outward from the face along a C–H bond (Figure 2), in agreement with previous observations.<sup>28,30–33</sup> Selected optimized distances of the resulting C<sub>s</sub> symmetric complex **2A** are given in Table 1.

Comparing the results obtained using both the B3LYP and MP2 methods with the aug-cc-pVTZ basis set enables evaluation of the applicability of the former method for such systems. The MP2 method predicts that upon binding to C<sub>6</sub>H<sub>6</sub> the bond length of the NO moiety ( $r(\text{N–O})$ ) lengthens by 0.043 Å to 1.125 Å. Indeed, it is now only marginally shorter than the bond length of isolated  $\bullet\text{NO}$  (Table 2). Thus, the complex formed resembles

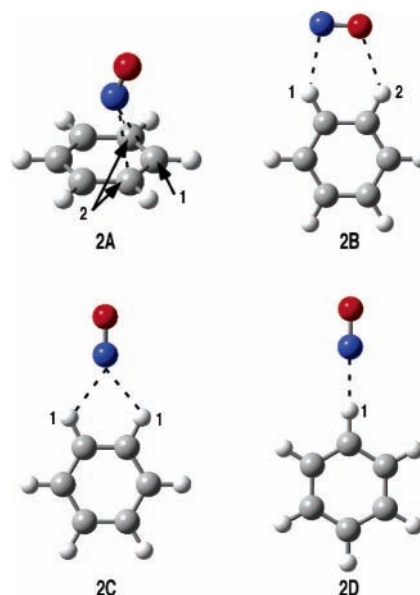


**Figure 2.** Schematic illustration of the optimized structures of (**2A**) C<sub>6</sub>H<sub>6</sub> $\cdots\text{NO}^+$  and C<sub>6</sub>H<sub>6</sub> $\cdots\text{NO}^-$  with NO<sup>-</sup> bound side-on or N-end-on via (**2C**) two hydrogen bonds or (**2D**) one hydrogen bond: C (gray); N (blue); O (red); H (white).

**TABLE 1: Selected Optimized Distances (Å) and Complexation Energy (kJ mol<sup>-1</sup>) of C<sub>6</sub>H<sub>6</sub> $\cdots\text{NO}^+$  (**2A**) Obtained Using the B3LYP and MP2 Methods in Combination with a Range of Basis Sets**

level of theory		$r(\text{N–O})$	$r(\text{N}\cdots\text{C}_1)$	$r(\text{N}\cdots\text{C}_2)$	$\Delta E_{\text{corr}}$
B3LYP	6-311G(d,p)	1.100	2.476	2.546	193.7
	6-311+G(d,p)	1.101	2.469	2.542	189.9
	6-311G++(d,p)	1.101	2.469	2.543	190.0
	6-311G(df,p)	1.098	2.484	2.547	190.8
	6-311G(2d,p)	1.099	2.450	2.530	193.5
	6-311+G(2df,p)	1.097	2.452	2.534	186.5
	aug-cc-pVDZ	1.109	2.450	2.526	194.6
	aug-cc-pVTZ	1.097	2.446	2.533	187.2
	MP2	aug-cc-pVDZ	1.139	2.491	2.505
aug-cc-pVTZ		1.125	2.400	2.455	158.7

C<sub>6</sub>H<sub>6</sub><sup>++</sup> $\cdots\text{NO}$ , i.e., almost complete electron transfer (see Table S2 for atomic charges of all complexes). The B3LYP method also predicts  $r(\text{N–O})$  to lengthen by 0.04 Å upon complexation. However, it has lengthened to just 1.097 Å, midway between the bond lengths of NO<sup>+</sup> and  $\bullet\text{NO}$  as calculated at the same level of theory (Table 2). The resultant complex can thus be described as [C<sub>6</sub>H<sub>6</sub> $\cdots\text{NO}$ ]<sup>+</sup>, i.e., only partial electron transfer. It should be noted that B3LYP in combination with any basis set used in this present study gives  $r(\text{N–O})$  of NO<sup>+</sup> to be approximately 0.03 Å shorter than obtained at the MP2 level (Table 2). The experimental adiabatic ionization energies (IEs) of C<sub>6</sub>H<sub>6</sub> and NO are close at 891.9 and 893.9 kJ mol<sup>-1</sup>, respectively.<sup>42</sup> Hence, upon interaction an equal sharing of an electron might reasonably be expected as observed with the B3LYP method. It is noted that their IEs as calculated at the B3LYP/6-311G(2d,p) level differ by 65.4 kJ mol<sup>-1</sup> (Table 3). For the NO<sup>+</sup> $\cdots$ ring carbon distances  $r(\text{N}\cdots\text{C}_1)$  and  $r(\text{N}\cdots\text{C}_2)$ , the MP2 (2.400 and 2.455 Å) and B3LYP (2.446 and 2.533 Å) methods are in reasonable agreement, and the B3LYP method predicts moderately longer interactions (0.046 and 0.078 Å). It should be noted that previous computational studies on this complex<sup>28,31–33</sup> have reported  $r(\text{N}\cdots\text{C}_1)$  distances of 2.44–2.46 Å, in agreement with our DFT results. In addition, other studies on cation $\cdots\pi$  interactions have reported that the B3LYP method overestimates this interaction distance in comparison to the MP2

**TABLE 2: Optimized N–O Bond Distances (Å) for Nitric Oxide and Its Mono-Ions Obtained Using the B3LYP and MP2 Methods in Combination with a Range of Basis Sets**

level of theory		$r(\text{N–O})$		
method	basis set	NO <sup>+</sup>	*NO	NO <sup>-</sup>
B3LYP	6-311G(d,p)	1.060	1.148	1.273
	6-311+G(d,p)	1.060	1.148	1.264
	6-311++G(d,p)	1.060	1.148	1.264
	6-311G(df,p)	1.058	1.147	1.271
	6-311G(2d,p)	1.058	1.148	1.273
	6-311+G(2df,p)	1.057	1.146	1.262
	aug-cc-pVDZ	1.068	1.154	1.266
	aug-cc-pVTZ	1.057	1.146	1.259
	aug-cc-pVTZ	1.096	1.142	1.276
MP2	aug-cc-pVDZ	1.096	1.142	1.276
	aug-cc-pVTZ	1.082	1.137	1.265
exptl <sup>a</sup>			1.150	

<sup>a</sup> Reference 47.**TABLE 3: Calculated<sup>a</sup> Adiabatic Ionization Energies (IEs) (kJ mol<sup>-1</sup>) for NO, C<sub>6</sub>H<sub>6</sub>, and R-Groups<sup>b</sup> of the Aromatic Amino Acids and Corrected Complexation Energies (kJ mol<sup>-1</sup>) for the Ar···NO<sup>+/-</sup> and Ar···NO<sup>+/-</sup>···Ar Complexes**

species	IE	complexation energy			
		Ar···NO <sup>+</sup>	Ar···NO <sup>+</sup> ···Ar	Ar···NO <sup>-</sup>	Ar···NO <sup>-</sup> ···Ar
NO	931.5				
C <sub>6</sub> H <sub>6</sub>	866.1	186.3	219.2	24.1	49.5
Phe	822.3	205.6	243.5	25.6	59.0
Tyr	754.8	223.1	265.6	95.4	164.7
His	781.9	263.7	335.9	98.9	173.7
Trp	696.6	263.4	313.6	85.2	152.3

<sup>a</sup> B3LYP/6-311G(2d,p) + ZPVE. <sup>b</sup> See Figure 1.

method.<sup>43,44</sup> Importantly, however, both methods predict the same overall general structural features with the ON···C<sub>1</sub> interaction being the shorter of the two by 0.055 Å (MP2) and 0.087 Å (B3LYP).

A variety of basis sets were then used in conjunction with the B3LYP method (Table 1). As noted above, the B3LYP method with all basis sets gives shorter  $r(\text{N–O})$  distances than obtained using the MP2 method while consistently overestimating the  $r(\text{N}\cdots\text{C}_1)$  and  $r(\text{N}\cdots\text{C}_2)$  distances. For example, with the smallest basis set used in this present study, 6-311G(d,p),  $r(\text{N}\cdots\text{C}_1)$  and  $r(\text{N}\cdots\text{C}_2)$  are 0.076 and 0.091 Å longer, respectively, than obtained at the MP2/aug-cc-pVTZ level. Only minor changes of less than 0.01 Å are observed upon inclusion of diffuse or f-functions on heavy atoms, 6-311+G(d,p) or 6-311G(df,p), respectively, or upon addition of diffuse functions on the hydrogen atoms, 6-311++G(d,p). Slightly larger effects are observed upon inclusion of a second set of d-functions, 6-311G(2d,p), with modest shortenings in both  $\text{N}\cdots\text{C}_1$  and  $\text{N}\cdots\text{C}_2$  by 0.026 and 0.016 Å to 2.450 and 2.530 Å, respectively. In fact, the resulting bond lengths are now in close agreement with those obtained at the B3LYP/aug-cc-pVDZ level (Table 1). Combining these individual enhancements to give the 6-311+G(2df,p) basis set does not significantly improve  $r(\text{N}\cdots\text{C}_1)$  (2.452 Å) or  $r(\text{N}\cdots\text{C}_2)$  (2.534 Å) further.

Thus, for the B3LYP method the 6-311G(2d,p), 6-311+G(2df,p), and aug-cc-pVDZ basis sets appear to provide the most reliable overall geometries. While the latter does give slightly more accurate geometries, the differences are not significant. In addition, Pople basis sets are more computationally feasible for larger sandwich complexes. Hence, optimized geometries of all further complexes with NO<sup>+</sup> were obtained at the B3LYP/6-311G(2d,p) level of theory.

Complexation energies ( $\Delta E_{\text{corr}}$ ) for [C<sub>6</sub>H<sub>6</sub>···NO]<sup>+</sup> were also determined at each level of theory employed (Table 1).

**TABLE 4: Selected Optimized Distances (Å) and Complexation Energy (kJ mol<sup>-1</sup>) Obtained at Various Levels of Theory for the NO<sup>-</sup> Bound Side-On C<sub>6</sub>H<sub>6</sub>···NO<sup>-</sup> Complex 2B**

level of theory		$r(\text{N–O})$	$r(\text{N}\cdots\text{H}_1)$	$r(\text{O}\cdots\text{H}_2)$	$\Delta E_{\text{corr}}$
method	basis set				
B3LYP	6-311G(d,p)	1.260	2.275	2.254	48.4
	6-311+G(d,p)	1.260	2.379	2.372	29.3
	6-311++G(d,p)	1.259	2.377	2.383	24.7
	6-311G(df,p)	1.258	2.276	2.262	37.4
	6-311G(2d,p)	1.261	2.278	2.263	37.4
	6-311+G(2df,p)	1.257	2.347	2.427	32.1
	aug-cc-pVDZ	1.261	2.309	2.468	21.9
	aug-cc-pVTZ	1.241	2.417	2.585	17.4
	aug-cc-pVTZ	1.276	2.251	2.366	36.9
MP2	aug-cc-pVTZ	1.265	2.268	2.308	25.2

Compared to that obtained at the MP2/aug-cc-pVTZ level (158.7 kJ mol<sup>-1</sup>), for all basis sets presently used B3LYP consistently overestimates  $\Delta E_{\text{corr}}$  by 27.8–35.9 kJ mol<sup>-1</sup> with the B3LYP/6-311+G(2df,p) level giving the closest agreement (186.5 kJ mol<sup>-1</sup>). Thus,  $\Delta E_{\text{corr}}$  for all further complexes involving NO<sup>+</sup> was obtained by performing single point energy calculations at this level of theory using B3LYP/6-311G(2d,p) optimized geometries, i.e., B3LYP/6-311+G(2df,p)/B3LYP/6-311G(2d,p) (Table 1). Indeed, we note that this approach gives the  $\Delta E_{\text{corr}}$  of [C<sub>6</sub>H<sub>6</sub>···NO]<sup>+</sup> to be 186.3 kJ mol<sup>-1</sup> (Table 3).

**3.3. C<sub>6</sub>H<sub>6</sub>···NO<sup>-</sup> Complexes.** In the interaction of NO<sup>-</sup> with C<sub>6</sub>H<sub>6</sub>, no anion··· $\pi$  complexes were obtained; instead it only binds by forming hydrogen bonds. Several complexes are possible depending on whether one or two hydrogens of C<sub>6</sub>H<sub>6</sub> are involved and the relative orientation of the NO<sup>-</sup> moiety. At all levels of theory used in this study, the lowest energy complex (**2B**) corresponds to NO<sup>-</sup> binding side-on to C<sub>6</sub>H<sub>6</sub> via two hydrogens (Figure 2). Selected optimized distances obtained using the MP2 and B3LYP methods with a variety of basis sets are listed in Table 4.

Several differences can be seen upon comparing the optimized structures of **2B** obtained using both the MP2 and B3LYP methods with the aug-cc-pVTZ basis set. In particular, MP2 predicts no shortening of the N–O bond upon complexation, whereas with B3LYP it shortens by 0.018 Å to 1.241 Å. While both methods predict similar structural characteristics with the  $\text{N}\cdots\text{H}_1\text{C}$  hydrogen bond being shorter than the  $\text{O}\cdots\text{H}_2\text{C}$  hydrogen bond, for MP2  $r(\text{N}\cdots\text{H}_1\text{C})$  is only 0.040 Å shorter, whereas for B3LYP it is less by 0.168 Å. More importantly perhaps, the B3LYP method predicts both interactions to be significantly longer by 0.149 and 0.277 Å, respectively, than obtained at the corresponding MP2 level.

Interestingly, when Pople rather than Dunning basis sets are used in combination with the B3LYP method, the results are in closer agreement with those obtained at the MP2/aug-cc-pVTZ level. In particular, when diffuse functions are *not included* in the basis set, i.e., 6-311G(d,p), 6-311G(df,p), and 6-311G(2d,p), the  $\text{N}\cdots\text{H}_1\text{C}$  hydrogen-bond distances are 2.275–2.278 Å, i.e., just slightly longer by 0.007–0.010 Å. Furthermore, these basis sets also give the second hydrogen-bond lengths,  $r(\text{O}\cdots\text{H}_2\text{C})$ , to be only 0.045–0.054 Å shorter than at the MP2/aug-cc-pVTZ level. In addition, the N–O bond shortens upon complexation by 0.012–0.013 Å. In contrast, the B3LYP method in combination with Pople basis sets that *do include* diffuse functions, i.e., 6-311+G(d,p), 6-311++G(d,p), and 6-311+G(2df,p), predicts lengths of both the  $\text{N}\cdots\text{H}_1\text{C}$  and  $\text{O}\cdots\text{H}_2\text{C}$  hydrogen bonds to be markedly longer than obtained at the MP2/aug-cc-pVTZ level by 0.079–0.111 and 0.064–0.119 Å, respectively. Reflecting the now weaker interaction between NO<sup>-</sup> and C<sub>6</sub>H<sub>6</sub>, the N–O

**TABLE 5: Selected Optimized Distances (Å) and Complexation Energies (kJ mol<sup>-1</sup>) Obtained at Various Levels of Theory for the NO<sup>-</sup> Bound N-End-On C<sub>6</sub>H<sub>6</sub>⋯NO<sup>-</sup> Complex**

level of theory		<i>r</i> (N–O)	<i>r</i> (N⋯H <sub>1</sub> )	$\Delta E_{\text{corr}}$
method	basis set			
B3LYP	6-311G(d,p) <sup>a</sup>	1.243	2.366	37.3
	6-311+G(d,p) <sup>a</sup>	1.250	2.490	31.2
	6-311++G(d,p) <sup>a</sup>	1.249	2.493	27.6
	6-311G(df,p) <sup>a</sup>	1.241	2.365	37.4
	6-311G(2d,p) <sup>a</sup>	1.243	2.367	36.1
	6-311+G(2df,p) <sup>a</sup>	1.247	2.497	26.5
	aug-cc-pVDZ <sup>b</sup>	1.252	2.100	15.7
MP2	aug-cc-pVTZ <sup>b</sup>	1.232	2.256	13.8
	aug-cc-pVDZ <sup>a</sup>	1.271	2.409	33.1
	aug-cc-pVTZ <sup>a</sup>	1.260	2.396	21.3

<sup>a</sup> Optimized as **2C** in Figure 2. <sup>b</sup> Optimized as **2D** in Figure 2.

bond is concomitantly predicted to shorten by just 0.004–0.005 Å upon complexation. It is generally thought that diffuse functions should improve the accuracy of anionic structures. In this case, however, it appears that the inclusion of such functions causes an erroneous overestimation of such long, weak intermolecular interactions by the B3LYP method.

An alternative C<sub>6</sub>H<sub>6</sub>⋯NO<sup>-</sup> complex with NO<sup>-</sup> bound end-on via its nitrogen to C<sub>6</sub>H<sub>6</sub> was found to lie just a few kJ mol<sup>-1</sup> higher in energy at all levels of theory. Selected optimized distances for the resulting C<sub>2v</sub> symmetric complexes **2C** and **2D** (Figure 2) are listed in Table 5. At the MP2/aug-cc-pVTZ level the NO<sup>-</sup> binds via two hydrogen bonds (**2C**) of length 2.396 Å and now has an N–O bond length of 1.260 Å. In contrast, at the corresponding B3LYP/aug-cc-pVTZ level NO<sup>-</sup> binds via a single (**2D**) considerably shorter (2.256 Å) hydrogen bond and has a shorter N–O bond of length 1.232 Å. We note that **2D** was only obtained when using Dunning basis sets used in combination with the B3LYP method. Analogous to that observed for **2B**, when Pople basis sets are used, there is a marked geometric sensitivity to the inclusion of diffuse functions on heavy atoms. As can be seen in Table 5, those that *do not include* such functions give optimized *r*(N⋯H<sub>1</sub>) values in the narrow range 2.365–2.367 Å and just 0.03 Å shorter than obtained at the MP2/aug-cc-pVTZ level. In contrast, those that *do include* such functions give *r*(N⋯H<sub>1</sub>) values that are decidedly longer by 0.094–0.101 Å, in the range 2.490–2.497 Å.

Considering the results obtained for both side-on and end-on C<sub>6</sub>H<sub>6</sub>⋯NO<sup>-</sup> complexes, the B3LYP/6-311G(2d,p) level of theory was chosen to obtain all further optimized structures for complexes involving NO<sup>-</sup>. As can be seen from Tables 4 and 5, the calculated complexation energies ( $\Delta E_{\text{corr}}$ ) for **2B** and **2C** are particularly sensitive to the inclusion of diffuse functions on *both* heavy and hydrogen atoms with decreases of 6.1–23.7 kJ mol<sup>-1</sup> upon their inclusion. However,  $\Delta E_{\text{corr}}$  for the anionic complex **2B** is also sensitive to a set of f- or second set of d-functions on heavy atoms with observed decreases in  $\Delta E_{\text{corr}}$  of 11.0 kJ mol<sup>-1</sup> for both upon their inclusion (Table 4). Thus, for all further anionic complexes  $\Delta E_{\text{corr}}$  was obtained by performing single point calculations at the B3LYP/6-311++G(2df,p)/B3LYP/6-311G(2d,p) level of theory. Indeed, we note that at this level of theory the complexation energy for **2B** is 24.1 kJ mol<sup>-1</sup> (Table 3), in close agreement with that obtained at the MP2/aug-cc-pVTZ level.

**3.4. Ar⋯NO<sup>+</sup> Complexes.** The aromatic R-groups (Ar) of the amino acids phenylalanine (Phe), tyrosine (Tyr), histidine (His), and tryptophan (Trp), Figure 1, were then allowed to interact with NO<sup>+</sup> in order to investigate the resulting structures

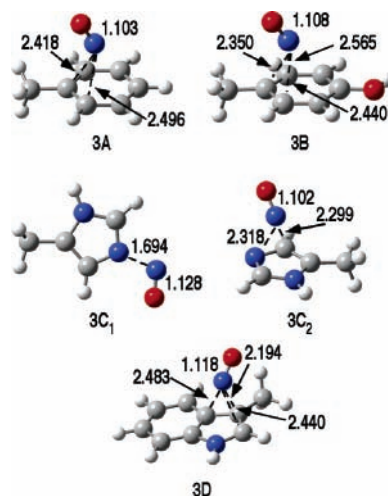


**Figure 3.** Optimized structures (B3LYP/6-311G(2d,p)) with selected distances (Å) for the Ar⋯NO<sup>+</sup> complexes where Ar is (**3A**) Phe, (**3B**) Tyr, (**3C<sub>1</sub>**) His with NO<sup>+</sup> bound via a ring nitrogen's lone pair, (**3C<sub>2</sub>**) His with NO<sup>+</sup> bound via its  $\pi$ -system, and (**3D**) Trp: C (gray); N (blue); O (red); H (white).

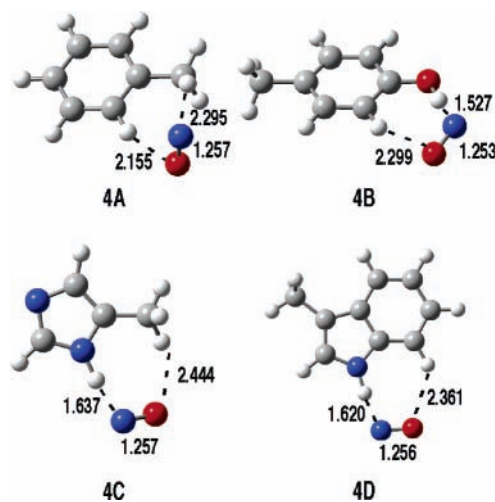


**Figure 4.** Optimized structures (B3LYP/6-311G(2d,p)) with selected distances (Å) for the lowest energy Ar⋯NO<sup>-</sup> complexes where Ar is (**4A**) Phe, (**4B**) Tyr, (**4C**) His, and (**4D**) Trp: C (gray); N (blue); O (red); H (white).

and complexation energies. Unless noted, only the lowest energy complex for each is described with optimized structures and selected distances shown in Figure 3.

**3.4.1. Phe⋯NO<sup>+</sup>.** Similar to that for C<sub>6</sub>H<sub>6</sub>, the resulting complex (**3A**) is C<sub>s</sub> symmetric. The NO<sup>+</sup> moiety is centered over the alkylated end of the ring with its oxygen directed up and out from the ring face along the C–CH<sub>3</sub> bond, in agreement with previous observations.<sup>31</sup> The alkylated ring carbon is the most negatively charged in neutral toluene (Table S2), our model for Phe. Furthermore, it will provide the greatest stabilization of any positive charge buildup on the ring upon complexation. The N–O distance in **3A** is 1.103 Å, 0.045 Å longer than obtained for isolated NO<sup>+</sup> at the same level of theory (cf. Table 2) and again indicating only partial electron transfer from the aromatic group upon complexation. It is also slightly longer than observed in C<sub>6</sub>H<sub>6</sub>⋯NO<sup>+</sup>, in agreement with the fact that the IE of Phe is lower than that of C<sub>6</sub>H<sub>6</sub> (Table 3). As a result, NO<sup>+</sup> binds more strongly to Phe than C<sub>6</sub>H<sub>6</sub> as illustrated by the shorter ON⋯C1 (2.418 Å) and ON⋯C2 (2.496 Å) distances, respectively, and the modestly larger complexation energy of 205.6 kJ mol<sup>-1</sup> (Table 3).

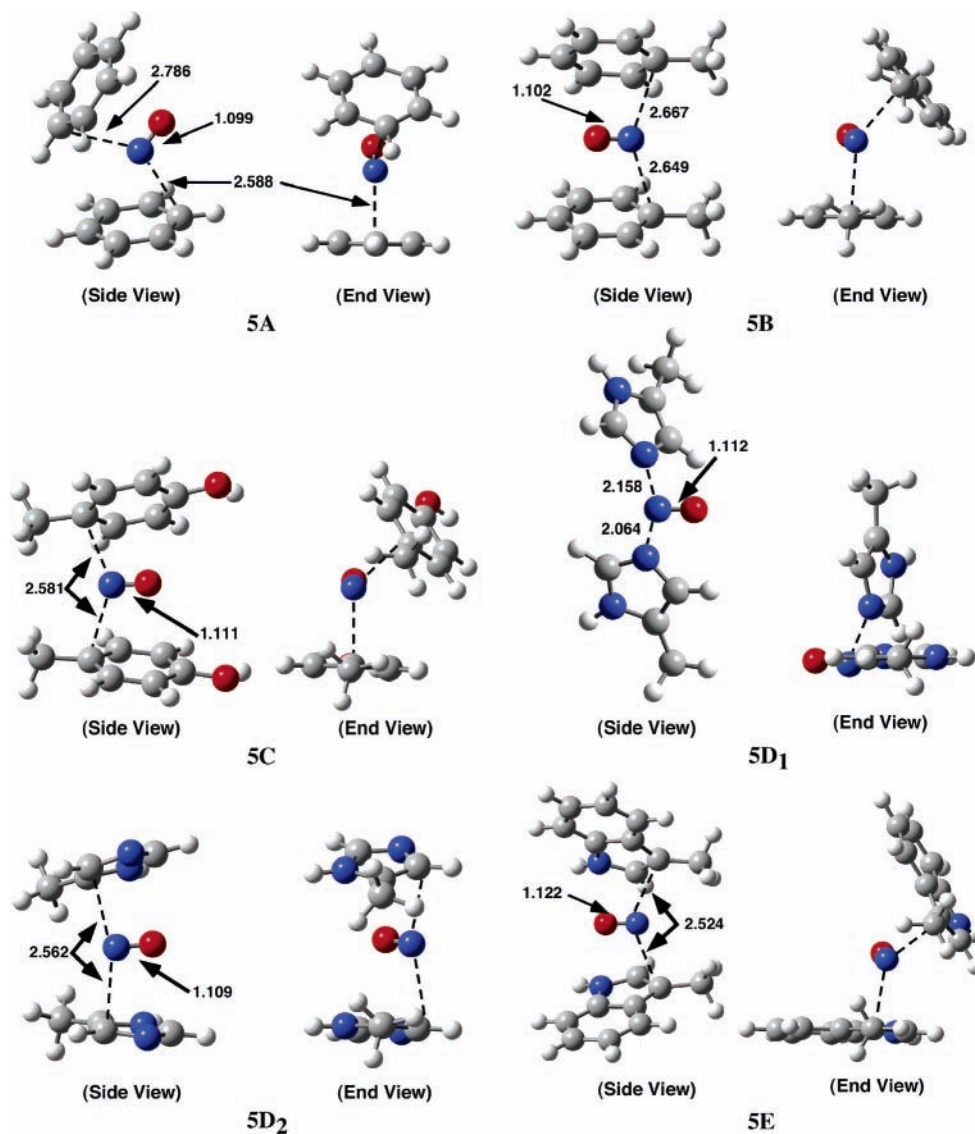


**Figure 5.** Optimized structures (B3LYP/6-311G(2d,p)) with selected distances (Å) of the  $[\text{Ar}\cdots\text{NO}\cdots\text{Ar}]^+$  complexes where Ar is (**5A**)  $\text{C}_6\text{H}_6$ , (**5B**) Phe, (**5C**) Tyr, (**5D**<sub>1</sub>) His when bound via both ring nitrogens' lone-pairs, (**5D**<sub>2</sub>) His when bound via both rings'  $\pi$ -systems, and (**5E**) Trp: C (gray); N (blue); O (red); H (white).

**3.4.2. Tyr $\cdots\text{NO}^+$ .** The resulting lowest energy complex (**3B**) is similar to that with Phe (**3A**) in that  $\text{NO}^+$  preferentially binds nearly centered over the alkylated end of the ring face with its oxygen directed up and away from the face almost parallel to the C–CH<sub>3</sub> bond. Interestingly, this is despite the fact that tyrosine contains an –OH group. Indeed, a complex was found in which the  $\text{NO}^+$  sits atop, almost parallel with the C–OH bond with its nitrogen over the –OH oxygen. However, such a complex is found to in fact lie 33.0 kJ mol<sup>-1</sup> higher in energy (Table S3). The IE of Tyr is calculated to be 67.5 kJ mol<sup>-1</sup> lower than that of Phe (Table 3). Consequently,  $r(\text{N}–\text{O})$  is now slightly longer than observed for **3A** while conversely the  $\text{ON}\cdots\text{C1}$  (2.350 Å) and  $\text{ON}\cdots\text{C2}$  (2.440 Å) interactions are now shorter by 0.068 and 0.056 Å, respectively. We note that the  $\text{ON}\cdots\text{C2}'$  distance (2.565 Å) is longer due to the fact that the  $\text{NO}^+$  is slightly off center. In addition, the complexation energy for **3B** is also 17.5 kJ mol<sup>-1</sup> larger at 223.1 kJ mol<sup>-1</sup> (Table 3).

**3.4.3. His $\cdots\text{NO}^+$ .** Histidine is an electron poor  $\pi$ -system due to the two nitrogens within the ring, one of which (denoted as N<sub>1</sub>) has a free electron lone-pair in the plane of the ring. Indeed, in the lowest energy complex formed (**3C**<sub>1</sub>)  $\text{NO}^+$  binds via its nitrogen center with this lone-pair resulting in a quite strong  $\text{N1}\cdots\text{NO}^+$  interaction of 1.694 Å. Also,  $r(\text{N}–\text{O})$  itself has

lengthened considerably to 1.128 Å, indicative of significant electron transfer from His to the  $\text{NO}^+$  moiety. In contrast, the  $\pi$ -bound complex **3C**<sub>2</sub> lies 49.6 kJ mol<sup>-1</sup> higher in energy (Table S3), with the  $\text{NO}^+$  moiety sitting 2.3 Å above the ring face with an N–O bond length of 1.102 Å, i.e., less electron transfer from His. The preference for the N1-bound complex is in agreement with previous observations on pyridine $\cdots\text{NO}^+$  interactions.<sup>28,32</sup> The complexation energy of **3C**<sub>1</sub> is 263.7 kJ mol<sup>-1</sup> (Table 3), the largest of all  $\text{Ar}\cdots\text{NO}^+$  complexes considered in this study. While the IE of the aromatic group of histidine is lower (Table 3) than that of  $\text{C}_6\text{H}_6$  and Phe but higher than that of Tyr, it should be noted that it corresponds to ionization from its  $\pi$ -system. Indeed, **3C**<sub>2</sub> has a lower complexation energy than **3B** as predicted.

**3.4.4. Trp $\cdots\text{NO}^+$ .**  $\text{NO}^+$  preferentially interacts via the alkylated carbon (C<sub>1</sub>) of the pyrrole ring with an  $\text{N}\cdots\text{C1}$  distance of 2.194 Å to give the  $\pi$ -bound complex **3D**. In addition, its own N–O bond has lengthened by 0.060 Å to 1.118 Å. The former distance is the shortest interaction observed for any of the  $\pi$ -complexes considered in this present study, while the latter is the largest lengthening observed upon complexation. This is due to the fact that the tryptophan's aromatic group has the lowest IE of all aromatic groups considered; thus, there is greater

electron transfer to the  $\text{NO}^+$  moiety, which is now also bound more tightly. Indeed, the complexation energy for **3D** is  $263.4 \text{ kJ mol}^{-1}$  (Table 3), the highest of all of the  $\pi$ -bound complexes considered and only  $0.3 \text{ kJ mol}^{-1}$  lower than that of the N1-bound histidine $\cdots\text{NO}^+$  complex **5D<sub>1</sub>**. An alternate complex lying only  $10.0 \text{ kJ mol}^{-1}$  higher in energy was found in which the  $\text{NO}^+$  was bound via the  $\pi$ -system of the six-membered ring of the Trp aromatic group (not shown). This is in contrast to previous studies<sup>45,46</sup> that found such a  $\pi$ -bound complex to in fact be preferred. We note, however, that these prior studies modeled the peptide backbone simply by using hydrogen. Thus, charge stabilization by the C1 center of tryptophan's aromatic group may have been underestimated.

**3.5.  $\text{Ar}\cdots\text{NO}^-$  Complexes.** Optimized structures for the  $\text{Ar}\cdots\text{NO}^-$  ( $\text{Ar} = \text{Phe, Tyr, His, Trp}$ ) complexes with selected distances obtained at the B3LYP/6-311G(2d,p) level are shown in Figure 4.

Unlike the cationic complexes, all of the lowest energy  $\text{Ar}\cdots\text{NO}^-$  complexes exhibit similar intramolecular binding. Specifically,  $\text{NO}^-$  forms two hydrogen bonds with each aromatic species; its nitrogen binds via the strongest donor while its oxygen binds via the next best "spatially available" donor. For example, in the  $\text{Phe}\cdots\text{NO}^-$  complex (**4A**) the  $\text{NO}^-$  nitrogen binds ( $2.295 \text{ \AA}$ ) via a hydrogen of the  $-\text{CH}_3$  group while the oxygen forms a shorter hydrogen bond ( $2.155 \text{ \AA}$ ) with the adjacent ring C2-H moiety. In addition, the N-O bond itself has now shortened by  $0.016 \text{ \AA}$  to  $1.257 \text{ \AA}$  (cf. Table 2). The calculated complexation energy for **4A** is  $25.6 \text{ kJ mol}^{-1}$ , just  $2.4 \text{ kJ mol}^{-1}$  larger than calculated for the  $\text{C}_6\text{H}_6\cdots\text{NO}^-$  complex **2B**. For the corresponding complex with tyrosine (**4B**) the  $\text{NO}^-$  nitrogen forms quite a short and strong hydrogen bond ( $1.527 \text{ \AA}$ ) with the tyrosyl's  $-\text{OH}$  group. Concomitantly, the  $\text{NO}^-$  oxygen forms a considerably weaker and longer bond ( $2.299 \text{ \AA}$ ) with a nearby ring C-H group (Figure 4). The N-O bond itself has also shortened slightly to  $1.253 \text{ \AA}$ . Because of the greater hydrogen-bond donor capabilities of tyrosine's  $-\text{OH}$  group, the complexation energy for **4B** is  $95.4 \text{ kJ mol}^{-1}$ , almost 4 times greater than that for the analogous complexes with  $\text{C}_6\text{H}_6$  and Phe (Table 3).

Similar to that described for the  $\text{Tyr}\cdots\text{NO}^-$  complex, upon interacting with histidine, the  $\text{NO}^-$  nitrogen forms a short strong bond with its best hydrogen-bond donor, the ring  $-\text{NH}-$  group. It is noted that in the resulting complex **4C** this bond is now longer ( $1.637 \text{ \AA}$ ) than the analogous bond in **4B** (Figure 4). Similarly, the  $\text{NO}^-$  oxygen forms a weaker, longer hydrogen bond ( $2.444 \text{ \AA}$ ) with a hydrogen of the nearby  $-\text{CH}_3$  group. Despite these longer distances, however, the complexation energy for **4C** is slightly higher than that of **4B** at  $98.9 \text{ kJ mol}^{-1}$  (Table 3). Similarly, with the aromatic group of tryptophan the  $\text{NO}^-$  nitrogen forms a short hydrogen bond ( $1.620 \text{ \AA}$ ) with its  $-\text{NH}-$  group (**4D**) while its oxygen forms a longer hydrogen bond with a nearby ring  $-\text{CH}-$  hydrogen. We note that at the present level of theory the  $\text{NO}^-$  oxygen prefers to interact with a  $-\text{CH}-$  group of the six-membered ring of the tryptophan's aromatic group with an  $\text{O}\cdots\text{HC}$  distance of  $2.592 \text{ \AA}$ . However, the alternate complex in which it interacts instead with a  $-\text{CH}-$  hydrogen of the five-membered ring lies just  $1.5 \text{ kJ mol}^{-1}$  higher in energy. The complexation energy of **4D** is  $85.2 \text{ kJ mol}^{-1}$ ,  $13.7 \text{ kJ mol}^{-1}$  lower than for **4C** (Table 3).

**3.6.  $[\text{Ar}\cdots\text{NO}\cdots\text{Ar}]^+$  Complexes.** After the studies on the "half-sandwiches", we then considered "full-sandwich" complexes, specifically those in which both aromatic species are the same. Optimized structures and selected bond distances obtained at the B3LYP/6-311G(2d,p) level are shown in Figure

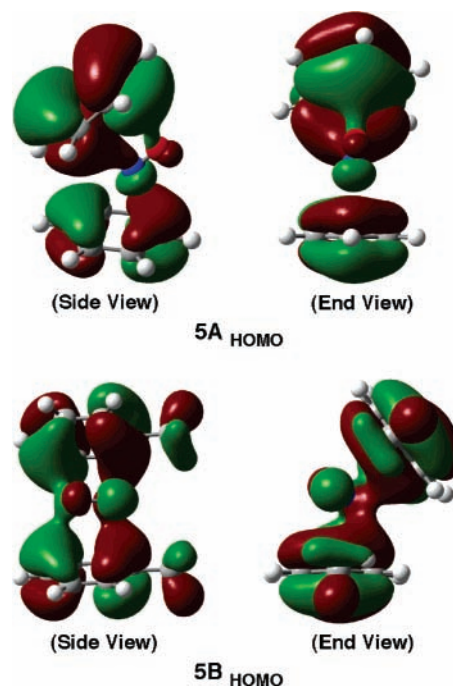


**Figure 6.** The highest occupied molecular orbital (HOMO) for the optimized structures of the  $\text{Ar}\cdots\text{NO}^+\cdots\text{Ar}$  sandwich complexes where Ar is (**5A<sub>HOMO</sub>**)  $\text{C}_6\text{H}_6$  and (**5B<sub>HOMO</sub>**) Phe: C (gray); N (blue); O (red); H (white).

5. For simplicity, except for histidine only the lowest energy complex is shown.

Interestingly, the cationic sandwich complexes do not correspond to a simple "doubling" of the half-sandwiches. For example, in **5A** the two  $\text{C}_6\text{H}_6$  rings bind to opposite sides of the  $\text{NO}^+$  with one tilted markedly toward the other perpendicular to the  $\text{NO}$  bond, coming closest to each other at the nitrogen end of  $\text{NO}^+$  (Figure 5). As a result, the  $\text{NO}^+$  does not sit directly between the two rings nor is its distance to both rings equal. With respect to the more closely bound  $\text{C}_6\text{H}_6$ , the  $\text{NO}^+$  sits in the same position and orientation as observed in the corresponding half-sandwich **2A**: centered over one end of the ring with its oxygen directed up and outward from the face. The distance from the  $\text{NO}^+$  nitrogen to the nearest ring carbon ( $r_{\text{ring}}$ ) is  $2.588 \text{ \AA}$ . In contrast, the second  $\text{C}_6\text{H}_6$  is orientated such that the  $\text{NO}^+$  effectively sits above its face, with its closest  $r_{\text{ring}}\cdots\text{NO}$  distance being significantly longer at  $2.786 \text{ \AA}$ . While both of these  $r_{\text{ring}}\cdots\text{NO}$  distances are notably longer than in **2A** (cf. Table 1), their combined effects result in  $r(\text{N}-\text{O})$  of **5A** being equal to that in **2A**, indicating a similar overall extent of electron transfer to the  $\text{NO}^+$  moiety (cf. Table 2). From Figure 6 it can be seen that the HOMO of **5A** (**5A<sub>HOMO</sub>**) corresponds to the two  $\text{C}_6\text{H}_6$  rings interacting with the same antibonding  $\pi$ -orbital on  $\text{NO}^+$ , one from above and the other below, in particular via its nitrogen.

The Phe (**5B**) and Tyr (**5C**) sandwiches, while possessing some similarities to their respective parent half-sandwiches **3A** and **3B** and the analogous  $\text{C}_6\text{H}_6$ -sandwich **5A**, exhibit a number of important differences. In both complexes the closest interactions again occur between the  $\text{NO}^+$  nitrogen and the alkylated ring carbons (C1) of each aromatic species with the distances to the tyrosine rings again being shorter than to the phenyl-alanine rings. In **5B** these distances are again unequal although now they differ by just  $0.018 \text{ \AA}$  (Figure 5). In contrast, in **5C** the  $\text{NO}^+$  sits equidistant from both rings with  $\text{C1}\cdots\text{NO}$  distances of  $2.581 \text{ \AA}$ . Significantly, however, in both complexes the  $\text{NO}^+$  moiety is now directed back over the faces of the rings involved

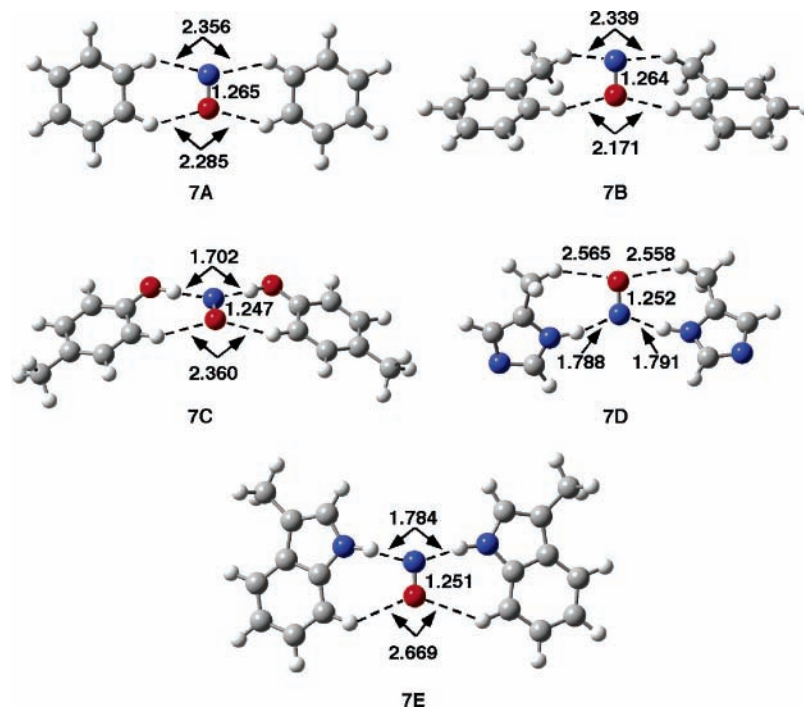


**Figure 7.** Optimized structures (B3LYP/6-311G(2d,p)) with selected distances (Å) of the  $[\text{Ar}\cdots\text{NO}\cdots\text{Ar}]^-$  complexes where Ar is (7A)  $\text{C}_6\text{H}_6$ , (7B) Phe, (7C) Tyr, (7D) His, and (7E) Trp: C (gray); N (blue); O (red); H (white).

rather than outward as in the corresponding half-sandwiches **3A** and **3B**, respectively (Figure 5). In addition, while the two rings in **5B** and **5C** are again tilted with respect to each other, the tilt axis is now essentially along the NO bond. As illustrated by the HOMO of the  $[\text{Phe}\cdots\text{NO}\cdots\text{Phe}]^+$  sandwich (**5B<sub>HOMO</sub>**) shown in Figure 6, this results in both rings now interacting with the *same* side of the antibonding  $\pi$ -orbital on  $\text{NO}^+$ . We note that as for **5A** and **2A**, despite the individually weaker  $\text{C1}\cdots\text{NO}$  interactions in **5B** and **5C**, the N–O lengths are in close agreement with those of their related half-sandwiches **3A** and **3B**, respectively.

When the aromatic group of a second histidine ( $\text{His}_b$ ) is allowed to interact with the lowest energy  $\text{His}_a\cdots\text{NO}^+$  complex **3C<sub>1</sub>**, it also preferentially binds with the nitrogen of the  $\text{NO}^+$  moiety via the lone-pair of its N1 center to give complex **5D<sub>1</sub>** (Figure 5). However, the  $\text{His}_b$  group sits almost perpendicular to the plane of the initial  $\text{His}_a\cdots\text{NO}^+$  moiety with a significantly longer (0.094 Å)  $\text{N1}\cdots\text{NO}^+$  distance than for the  $\text{His}_a$  ring. An alternate  $C_s$  symmetric sandwich-type complex (**5D<sub>2</sub>**) was also obtained in which the  $\text{NO}^+$  moiety is positioned over the  $-\text{CHN1CH}-$  component of each ring, its nitrogen being 2.562 Å from the ring carbons adjacent to the alkylated carbons (Figure 5). However, such a complex lies significantly higher in energy than **5D<sub>1</sub>** by 73.4  $\text{kJ mol}^{-1}$ . It should be noted that despite the structural differences between **5D<sub>2</sub>** and **5B/5C**, it possesses a similar HOMO with regards to orientation and mode of interaction between the aromatic rings and  $\text{NO}^+$  (Figure S1).

For the aromatic group of tryptophan, the lowest energy sandwich (**5E**) corresponds to  $\text{NO}^+$  interacting equally with both pyrrole rings, its closest contact being the  $\text{ON}\cdots\text{C1}$  (alkylated carbon) distance at 2.524 Å (Figure 5). Similar to that observed for sandwiches **5B** and **5C** formed by the aromatic groups of Phe and Tyr, respectively, the  $\text{NO}^+$  is directed back over the faces of the pyrrole rings. Furthermore, the tryptophan rings are also tilted with respect to each other such that they interact with the same lobes of a  $\pi$ -antibonding orbital of  $\text{NO}^+$  (Figure S1). Similarly, as for all other  $\text{Ar}\cdots\text{NO}^+\cdots\text{Ar}$  complexes considered (see Figure 5), the N–O bond lengthens upon

complexing with two aromatic species. However, as for the half-sandwiches, only partial charge transfer occurs (see Table S2) as illustrated by the fact that its length now lies between that of  $\text{NO}^+$  and  $\text{NO}^\bullet$  as calculated at the same level of theory (Table 2). The degree of charge transfer is dependent on the IE of the aromatic species involved.

The complexation energies ( $\Delta E_{\text{corr}}$ ) for the sandwich complexes of  $\text{NO}^+$  with  $\text{C}_6\text{H}_6$  (**5A**) and the aromatic groups of Phe (**5B**), Tyr (**5C**), and Trp (**5E**) are 219.2, 243.5, 265.6, and 313.6  $\text{kJ mol}^{-1}$ , respectively (Table 3). Comparison with  $\Delta E_{\text{corr}}$  of the half-sandwiches indicates that addition of a second appropriate aromatic group is increasingly favored by 32.9, 38.0, 42.4, and 50.2  $\text{kJ mol}^{-1}$ . Thus,  $\text{NO}^+$  prefers to form sandwiches with the side group of tryptophan compared to those of tyrosine and phenylalanine, with tyrosine being slightly preferred of these latter two. For the side group of histidine the preferred complex **5D<sub>1</sub>** has the highest  $\Delta E_{\text{corr}}$  at 335.9  $\text{kJ mol}^{-1}$  but is not a sandwich-type complex. The corresponding sandwich **5D<sub>2</sub>** has a much lower complexation energy of 262.5  $\text{kJ mol}^{-1}$  (Table S3), which in fact is also slightly lower than that of **5C**. It is noted that while in proteins the histidine side group is often protonated due to its  $\text{pK}_a$  being near 6, many metalloproteins use multiple unprotonated histidines to bind metal ions. Thus, the above results suggest that  $\text{NO}^+$  may in fact also be able to bind in such areas.

**3.7.  $[\text{Ar}\cdots\text{NO}\cdots\text{Ar}]^-$  Complexes.** Optimized structures for the anionic complexes with selected bond distances obtained at the B3LYP/6-311G(2d,p) level are shown in Figure 7. Unlike the cationic complexes, the lowest energy structure in all cases corresponds to a “doubling” of the parent half-complex in that the  $\text{NO}^-$  nitrogen and oxygen interact with the *same* hydrogens of *both* aromatic species as in the appropriate parent. For example, when  $\text{NO}^-$  interacts with two phenylalanine aromatic groups (**7B**), its nitrogen again interacts with a  $-\text{CH}_3$  hydrogen in each Phe group, while its oxygen interacts with a C–H adjacent to the alkylated carbon (C1) of each ring. All of the intermolecular interactions, however, are now longer than in their corresponding half-complexes by 0.018–0.308 Å. The

largest increase observed in any anionic complex except that involving the aromatic group of tryptophan (**7E**) occurs in the  $\text{ON}\cdots\text{HX}$  hydrogen bonds (Figure 7). It is noted that all of the resulting complexes except **7D**, involving the aromatic group of histidine, are symmetric at the present level of theory; i.e., the  $\text{NO}^-$  moiety sits equidistant from both aromatic species. In **7D** the  $\text{NO}^-$  is skewed slightly such that it forms a marginally shorter  $\text{N}-\text{H}\cdots\text{NO}$  bond with one of the histidine groups and simultaneously has a slightly shorter  $\text{NO}\cdots\text{H}-\text{C}$  bond with the other group. It is noted that no complexes involving  $\text{NO}^-\cdots\pi$  interactions were obtained.

The calculated complexation energies (Table 3) for  $\text{NO}^-$  interacting with two benzenes (**7A**) or aromatic groups of the amino acids phenylalanine (**7B**), tyrosine (**7C**), histidine (**7D**), and tryptophan (**7E**) are 49.5, 59.0, 164.7, 173.7, and 152.3  $\text{kJ mol}^{-1}$ , respectively. The overall order is the same as for the corresponding half-complexes. Clearly, there is a distinct preference by  $\text{NO}^-$  to form complexes with those groups that contain conventional hydrogen-bond donors such as  $-\text{OH}$  or  $\text{N}-\text{H}$  groups. Interestingly, **7A** and **7B**, which contain only  $\text{C}-\text{H}\cdots(\text{NO})^-$  interactions, give complexation energies that are slightly more than double those of their half-complexes **2B** and **4A**, respectively (see Table 3). In contrast, all others contain more conventional  $-\text{OH}\cdots\text{NO}$  or  $\text{N}-\text{H}\cdots\text{NO}$  hydrogen bonds and have complexation energies that are less than double those of their respective parent half-complexes.

#### 4. Conclusions

Complexes formed by the interaction of  $\text{NO}^+$  and  $\text{NO}^-$  with  $\text{C}_6\text{H}_6$  (benzene) and the aromatic R-groups of the amino acids phenylalanine (Phe), tyrosine (Tyr), histidine (His), and tryptophan (Trp) have been investigated. In particular, both the half- ( $\text{Ar}\cdots\text{NO}^{+/-}$ ) and full-sandwiches  $\text{Ar}\cdots\text{NO}^{+/-}\cdots\text{Ar}$  (where the Ar groups are the same) were studied. In addition, the reliability and accuracy of the B3LYP method for obtaining optimized structures and complexation energies for such complexes were also assessed by comparison with results obtained using the high-level ab initio method MP2/aug-cc-pVTZ.

In all  $\text{Ar}\cdots\text{NO}^+$  complexes considered,  $\text{NO}^+$  binds via its nitrogen center. Furthermore, except for the aromatic group of histidine, it preferentially binds via their  $\pi$ -system centered toward one end of the ring with its oxygen directed up and outward from the ring face parallel, or almost, with a  $\text{C}-\text{X}$  bond ( $\text{X} = \text{H}$ ,  $\text{Ar} = \text{C}_6\text{H}_6$ ;  $\text{X} = \text{CH}_3$ ,  $\text{Ar} = \text{Phe}$ ,  $\text{Tyr}$ ,  $\text{Trp}$ ). In contrast to previous studies,  $\text{NO}^+$  is found to prefer to bind via the pyrrole ring of tryptophan's aromatic group. For  $\text{Ar} = \text{His}$  the  $\text{ON}^+\cdots\pi$  complex lies 49.5  $\text{kJ mol}^{-1}$  higher in energy than when  $\text{NO}^+$  binds via the in-plane lone-pair of the histidine's ring nitrogen (N1). For the  $\text{Ar}\cdots\text{NO}^-$  complexes considered,  $\text{NO}^-$  binds side-on to the aromatic species via two hydrogen bonds. The lowest energy complexes correspond to the  $\text{NO}^-$  nitrogen binding with the aromatic's best hydrogen-bond donor while the oxygen binds to the next best "spatially available" donor.

The cationic  $\pi$ -sandwich complexes  $[\text{Ar}\cdots\text{NO}\cdots\text{Ar}]^+$  do not correspond to a "doubling" of their parent half-sandwiches. Except for  $\text{Ar} = \text{C}_6\text{H}_6$ , while the  $\text{NO}^+$  moiety again interacts via its nitrogen with the same ring atom as in the appropriate half-sandwich, it is now directed back over the face of the aromatic rings. Furthermore, for  $\text{Ar} = \text{C}_6\text{H}_6$  and the aromatic group of phenylalanine, at the level of theory used in this present study  $\text{NO}^+$  binds more closely to one of the aromatic rings than the other, the difference decreasing from  $\text{Ar} = \text{C}_6\text{H}_6$  to Phe. For  $\text{Ar} = \text{His}$ , the lowest energy cationic complex again

corresponds to both rings binding via their lone-pairs of the N1 ring centers to the  $\text{NO}^+$  nitrogen, although the rings are now almost perpendicular to each other. In contrast, the anionic  $[\text{Ar}\cdots\text{NO}\cdots\text{Ar}]^-$  complexes are found to correspond to a "doubling" of the parent  $\text{Ar}\cdots\text{NO}^-$  complexes with the same hydrogen-bond interactions being maintained.

The calculated complexation energies ( $\Delta E_{\text{corr}}$  values) for those complexes involving  $\text{NO}^+$  binding via the  $\pi$ -systems of the aromatic species indicate that it has a clear preference for the aromatic group of tryptophan. Indeed, for both half- and full-sandwich type complexes this preference is in the order  $\text{Trp} \gg \text{Tyr} > \text{His} > \text{Phe} > \text{C}_6\text{H}_6$ . For both types of complexes those involving the Trp aromatic group are favored by around 40  $\text{kJ mol}^{-1}$ . For the sandwich-type complexes the difference between  $\Delta E_{\text{corr}}$  for Tyr and His is quite small. The N1-bound  $\text{His}\cdots\text{NO}^+$  and  $\text{His}\cdots\text{NO}^+\cdots\text{His}$  complexes are both found to lie lower in energy than any of the  $\pi$ -bound complexes. Notably, however, the former is only quite marginally lower in energy than the  $\text{Trp}\cdots\text{NO}^+$  complex. For the anionic complexes, the calculated  $\Delta E_{\text{corr}}$  values indicate that  $\text{NO}^-$  strongly prefers those aromatic groups that contain conventional hydrogen-bond donor groups such as  $-\text{OH}$  or  $-\text{NH}-$ . For both types of complexes the order of preference is  $\text{His} > \text{Tyr} > \text{Trp} \gg \text{Phe} > \text{C}_6\text{H}_6$ .

**Acknowledgment.** We thank the Natural Sciences and Engineering Research Council of Canada (NSERC), Canadian Foundation for Innovation (CFI), and Ontario Innovation Trust (OIT) for funding and Sharcnet and the University of Waterloo for additional computational resources. C.B. and J.J.R. also thank the John and Anne Cristescu Memorial and Ontario Graduate (OGS) Scholarship programs, respectively, for financial support.

**Supporting Information Available:** Highest intramolecular bonding orbital for  $\text{NO}^+$  binding to two Ar rings in  $\text{Ar}\cdots\text{NO}^+\cdots\text{Ar}$  sandwich complexes, optimized xyz-coordinates, electronic energies ( $h$ ), ZPVE and BSSE corrections,  $\langle S^2 \rangle$  values, Mulliken atomic charges for all species considered in this study, and single point energy calculation results for  $\text{NO}^+$  and  $\text{NO}^-$  complexes and related species. This material is available free of charge via the Internet at <http://pubs.acs.org>.

#### References and Notes

- Gibaldi, M. *J. Clin. Pharmacol.* **1993**, *33*, 488.
- Rosen, G. M.; Tsai, P.; Pou, S. *Chem. Rev.* **2002**, *102*, 1191.
- Koshland, D. E. *Science* **1992**, *258*, 1861.
- Janssen, L. J.; Premji, M.; Lu-Chao, H.; Cox, G.; Keshavjee, S. *Am. J. Physiol.: Lung Cell. Mol. Physiol.* **2000**, *278*, 899.
- Fukuto, J. M.; Switzer, C. H.; Miranda, K. M.; Wink, D. A. *Annu. Rev. Pharmacol. Toxicol.* **2005**, *45*, 335.
- Butler, A. R.; Flitney, F. W.; Williams, D. L. H. *Trends Pharmacol. Sci.* **1995**, *16*, 18.
- Shiva, S.; Crawford, J. H.; Ramachandran, A.; Ceaser, E. K.; Hillson, T.; Brookes, P. S.; Patel, R. P.; Darley-Usmar, V. M. *Biochem. J.* **2004**, *379*, 359.
- Broillet, M.-C. *Cell. Mol. Life Sci.* **1999**, *55*, 1036.
- Al-Sa'doni, H.; Ferro, A. *Clin. Sci.* **2000**, *98*, 507.
- Gaston, B. *Biochim. Biophys. Acta* **1999**, *1411*, 323.
- Wang, K.; Zhang, W.; Xian, M.; Hou, Y.-C.; Chen, X.-C.; Cheng, J.-P.; Wang, P. G. *Curr. Med. Chem.* **2000**, *7*, 821.
- Akhter, S.; Vignini, A.; Wen, Z.; English, A.; Wang, P. G.; Mutus, B. *Proc. Natl. Acad. Sci. U.S.A.* **2002**, *99*, 9172.
- Meyer, E. A.; Castellano, R. K.; Diederich, F. *Angew. Chem., Int. Ed.* **2003**, *42*, 1210.
- Ma, J. C.; Dougherty, D. A. *Chem. Rev.* **1997**, *97*, 1303.
- Reddy, S. A.; Sastry, G. N. *J. Phys. Chem. A* **2005**, *109*, 8893.
- Gallivan, J. P.; Dougherty, D. A. *Proc. Natl. Acad. Sci. U.S.A.* **1999**, *96*, 9459.

- (17) Liu, T.; Zhu, W.; Gu, J.; Shen, J.; Luo, X.; Chen, G.; Puah, C. M.; Silman, I.; Chen, K.; Sussman, J. L.; Jiang, H. *J. Phys. Chem. A* **2004**, *108*, 9400.
- (18) Waters, M. L. *Biopolymers* **2004**, *76*, 435.
- (19) Garau, C.; Frontera, A.; Quiñero, D.; Ballester, P.; Costa, A.; Deya, P. M. *Chem. Phys. Lett.* **2004**, *392*, 85.
- (20) Mascal, M.; Armstrong, A.; Bartberger, M. D. *J. Am. Chem. Soc.* **2002**, *124*, 6274.
- (21) Hartmann, M.; Wetmore, S. D.; Radom, L. *J. Phys. Chem. A* **2001**, *105*, 4470.
- (22) Chaney, J. D.; Goss, C. R.; Foltz, K.; Santarsiero, B. D.; Hollingsworth, M. D. *J. Am. Chem. Soc.* **1996**, *118*, 9432.
- (23) Desiraju, G. R. *Acc. Chem. Res.* **1991**, *24*, 290.
- (24) Steiner, T.; Saenger, W. *J. Am. Chem. Soc.* **1992**, *114*, 10146.
- (25) Rosokha, S. V.; Kochi, J. K. *J. Am. Chem. Soc.* **2001**, *123*, 8985.
- (26) Rosokha, S. V.; Kochi, J. K. *J. Am. Chem. Soc.* **2002**, *124*, 5620.
- (27) Rosokha, S. V.; Lindeman, S. V.; Rathore, R.; Kochi, J. K. *J. Org. Chem.* **2003**, *68*, 3947.
- (28) Grabow, J. A. D.; Meyer, P. M. *Eur. J. Mass Spectrom.* **2004**, *10*, 899.
- (29) Zhao, Y.-L.; Bartberger, M. D.; Goto, K.; Shimada, K.; Kawashima, T.; Houk, K. N. *J. Am. Chem. Soc.* **2005**, *127*, 7964.
- (30) Gwaltney, S. R.; Rosokha, S. V.; Head-Gordon, M.; Kochi, J. K. *J. Am. Chem. Soc.* **2003**, *125*, 3273.
- (31) Skokov, S.; Wheeler, R. A. *J. Phys. Chem. A* **1999**, *103*, 4261.
- (32) Dechamps, N.; Gerbaux, P.; Flammang, R.; Bouchoux, G.; Nam, P. C.; Nguyen, M. T. *Int. J. Mass Spectrom.* **2004**, *232*, 31.
- (33) Chiavarino, B.; Crestoni, M. E.; Fornarini, S.; Lemaire, J.; Maitre, P.; MacAleese, L. *J. Am. Chem. Soc.* **2006**, *128*, 12553.
- (34) Frisch, M. J.; Trucks, G. W.; Schlegel, H. B.; Scuseria, G. E.; Robb, M. A.; Cheeseman, J. R.; Montgomery, J. A., Jr.; Vreven, T.; Kudin, K. N.; Burant, J. C.; Millam, J. M.; Iyengar, S. S.; Tomasi, J.; Barone, V.; Mennucci, B.; Cossi, M.; Scalmani, G.; Rega, N.; Petersson, G. A.; Nakatsuji, H.; Hada, M.; Ehara, M.; Toyota, K.; Fukuda, R.; Hasegawa, J.; Ishida, M.; Nakajima, T.; Honda, Y.; Kitao, O.; Nakai, H.; Klene, M.; Li, X.; Knox, J. E.; Hratchian, H. P.; Cross, J. B.; Bakken, V.; Adamo, C.; Jaramillo, J.; Gomperts, R.; Stratmann, R. E.; Yazyev, O.; Austin, A. J.; Cammi, R.; Pomelli, C.; Ochterski, J. W.; Ayala, P. Y.; Morokuma, K.; Voth, G. A.; Salvador, P.; Dannenberg, J. J.; Zakrzewski, V. G.; Dapprich, S.; Daniels, A. D.; Strain, M. C.; Farkas, O.; Malick, D. K.; Rabuck, A. D.; Raghavachari, K.; Foresman, J. B.; Ortiz, J. V.; Cui, Q.; Baboul, A. G.; Clifford, S.; Cioslowski, J.; Stefanov, B. B.; Liu, G.; Liashenko, A.; Piskorz, P.; Komaromi, I.; Martin, R. L.; Fox, D. J.; Keith, T.; Al-Laham, M. A.; Peng, C. Y.; Nanayakkara, A.; Challacombe, M.; Gill, P. M. W.; Johnson, B.; Chen, W.; Wong, M. W.; Gonzalez, C.; Pople, J. A. *Gaussian 03*, Gaussian, Inc.: Pittsburgh, PA, 2004.
- (35) Becke, A. D. *J. Chem. Phys.* **1993**, *98*, 1372.
- (36) Stephens, P. J.; Devlin, F. J.; Chabalowski, C. F.; Frisch, M. J. *J. Phys. Chem.* **1994**, *98*, 11623.
- (37) Lee, C.; Yang, W.; Parr, R. G. *Phys. Rev. B* **1988**, *37*, 785.
- (38) Seeger, R.; Pople, J. A. *J. Chem. Phys.* **1977**, *66*, 3045.
- (39) Bauernshmitt, R.; Ahlrichs, R. *J. Chem. Phys.* **1996**, *104*, 9047.
- (40) Boys, S. F.; Bernardi, F. *Mol. Phys.* **1970**, *19*, 553.
- (41) Simon, S.; Duran, M.; Dannenberg, J. J. *J. Chem. Phys.* **1996**, *105*, 11024.
- (42) Afeefy, H. Y.; Liebman, J. F.; Stein, S. E. Neutral Thermochemical Data. *NIST Chemistry WebBook*; NIST Standard Reference Database Number 69; National Institute of Standards and Technology: Gaithersburg, MD, June 2005.
- (43) Felder, C.; Jiang, H. L.; Zhu, W. L.; Chen, K. X.; Silman, I.; Botti, S. A.; Sussman, J. L. *J. Phys. Chem. A* **2001**, *105*, 1326.
- (44) Liu, T.; Gu, J.; Tan, X. J.; Zhu, W. L.; Luo, X. M.; Jiang, H. L.; Ji, R. Y.; Chen, K. X.; Silman, I.; Sussman, J. L. *J. Phys. Chem. A* **2001**, *105*, 5431.
- (45) Basch, H.; Stevens, W. J. *J. Mol. Struct.: THEOCHEM* **1995**, *338*, 303.
- (46) Mecozzi, S.; West, A. P., Jr.; Dougherty, D. A. *Proc. Natl. Acad. Sci. U.S.A.* **1996**, *93*, 10566.
- (47) Kawanami, N.; Ozeki, T.; Yagasaki, A. *J. Am. Chem. Soc.* **2000**, *122*, 1239.